

REPORT DOCUMENTATION PAGE

Form Approved
OMB No. 0704-0188

Public reporting burden for this collection of information is estimated to average 1 hour per response, including the time for reviewing instructions, searching existing data sources, gathering and maintaining the data needed, and completing and reviewing this collection of information. Send comments regarding this burden estimate or any other aspect of this collection of information, including suggestions for reducing this burden to Department of Defense, Washington Headquarters Services, Directorate for Information Operations and Reports (0704-0188), 1215 Jefferson Davis Highway, Suite 1204, Arlington, VA 22202-4302. Respondents should be aware that notwithstanding any other provision of law, no person shall be subject to any penalty for failing to comply with a collection of information if it does not display a currently valid OMB control number. **PLEASE DO NOT RETURN YOUR FORM TO THE ABOVE ADDRESS.**

1. REPORT DATE (DD-MM-YYYY) 27-01-2006		2. REPORT TYPE Journal Article		3. DATES COVERED (From - To)	
4. TITLE AND SUBTITLE Millimeter Wave Plasma Interferometry in the Near Field of a Hall Plasma Accelerator (PREPRINT)				5a. CONTRACT NUMBER	
				5b. GRANT NUMBER	
				5c. PROGRAM ELEMENT NUMBER	
6. AUTHOR(S) M.A. Cappelli & N. Gascon (Stanford University); William Hargus, Jr. (AFRL/PRSS)				5d. PROJECT NUMBER 10110011	
				5e. TASK NUMBER	
				5f. WORK UNIT NUMBER	
7. PERFORMING ORGANIZATION NAME(S) AND ADDRESS(ES) Air Force Research Laboratory (AFMC) AFRL/PRSS 1 Ara Drive Edwards AFB CA 93524-7013				8. PERFORMING ORGANIZATION REPORT NUMBER AFRL-PR-ED-JA-2006-071	
9. SPONSORING / MONITORING AGENCY NAME(S) AND ADDRESS(ES) Air Force Research Laboratory (AFMC) AFRL/PRS 5 Pollux Drive Edwards AFB CA 93524-7048				10. SPONSOR/MONITOR'S ACRONYM(S)	
				11. SPONSOR/MONITOR'S NUMBER(S) AFRL-PR-ED-JA-2006-071	
12. DISTRIBUTION / AVAILABILITY STATEMENT Approved for public release; distribution unlimited (AFRL-ERS-PAS-06-052)					
13. SUPPLEMENTARY NOTES Submitted for publication in Journal of Propulsion and Power					
14. ABSTRACT <p>Measurements are described of electron number density in the near field of a 200W Hall plasma accelerator using a 90 GHz microwave interferometer. The system is of a phase-bridge design, utilizing two signal arms from a fixed frequency source (one passing through the plasma) that recombine at two balanced mixers. A line-integrated electron density is obtained by comparing the in-phase and quadrature signals from the mixers. Measurements across chords through a "symmetric" plasma plume are Abel inverted to give the radial variation in the plasma density. The first direct non-intrusive measurements of the electron density in the near field of this source reveals structure not previously resolved with electrical probes. This interferometer is suitable for measuring time-dependent plasma density fluctuations offering non-intrusive information about plasma oscillations and instabilities in the near exit region where electrical probes are known to interfere with the discharge operation.</p>					
15. SUBJECT TERMS					
16. SECURITY CLASSIFICATION OF:			17. LIMITATION OF ABSTRACT	18. NUMBER OF PAGES	19a. NAME OF RESPONSIBLE PERSON
a. REPORT	b. ABSTRACT	c. THIS PAGE			Dr. William A Hargus, Jr.
Unclassified	Unclassified	Unclassified	A	25	19b. TELEPHONE NUMBER <i>(include area code)</i> N/A

Millimeter Wave Plasma Interferometry in the Near Field of a Hall Plasma Accelerator

(Preprint)

M.A. Cappelli[†] and N. Gascon

Mechanical Engineering Department, Stanford University, Stanford, California

William Hargus, Jr.

Electric Propulsion Laboratory, Air Force Research Laboratories, Edwards AFB, California

Abstract

Measurements are described of electron number density in the near field of a 200W Hall plasma accelerator using a 90 GHz microwave interferometer. The system is of a phase-bridge design, utilizing two signal arms from a fixed frequency source (one passing through the plasma) that recombine at two balanced mixers. A line-integrated electron density is obtained by comparing the in-phase and quadrature signals from the mixers. Measurements across chords through a “symmetric” plasma plume are Abel inverted to give the radial variation in the plasma density. The first direct non-intrusive measurements of the electron density in the near field of this source reveals structure not previously resolved with electrical probes. This interferometer is suitable for measuring time-dependent plasma density fluctuations offering non-intrusive information about plasma oscillations and instabilities in the near exit region where electrical probes are known to interfere with the discharge operation.

[†]Corresponding Author: Prof. Mark A. Cappelli, cap@stanford.edu, tel: 650-725-2020

I. Introduction

The electron density is an important property to characterize in $\mathbf{E} \times \mathbf{B}$ Hall discharges used as plasma accelerators for space propulsion. Hall discharges are quasi-neutral plasma devices, and together with a measurement of the spatially-resolved ion velocity [1], measurements of local electron density provide a means of characterizing the ion current distribution. When the measurements are made close to the exit plane of the discharge source (i.e., in the “near-field”), the ion velocity and plasma density also serve as a benchmark for discharge simulations as their values and spatial distribution are sensitive to the ionization process and the accelerating electric field. The most common methods of determining the ion density in the near-field of a Hall thruster discharge is through the use of either cylindrical Langmuir probes operated in current saturation mode [2] or guarded ion probes [3], both of which suffer from being intrusive and from uncertainties in their interpretation due to ion-enhanced secondary electron emission. A measurement of the time-average plasma density using probes in the near-field of Hall thrusters is at best reliable to an order of magnitude, and time-resolved measurements must account for the probe’s non-linear spectral response. On the other hand, the ease of interpretation and non-intrusive nature of microwave interferometry makes it an attractive choice for collecting electron density data. Microwave interferometry at centimeter wavelengths (e.g., 12-18 GHz) has been used to study the distant plume (far-field) region of a Hall thruster [4]. However, its use in studying the near-field is hampered by the limited spatial resolution that can be obtained because the beam waist when focused is at best a few wavelengths in diameter.

In this paper, we present results of measurements of path-integrated electron line density using millimeter wave interferometry in the near-field of a commercial Hall plasma thruster (BHT-200) [5]. When Abel inverted, these measurements reduce to the radial variation in the electron density [under ideal axisymmetric conditions](#). As described below, a 90 GHz (3.3 mm) phase-bridge interferometer provided modest spatial resolution (~ 7 mm) and was used to carry out lateral and axial surveys of the plasma line-density within a few discharge channel diameters (approximately 50 mm) of the exit plane of the thruster.

The phase-bridge design, with resolved in-phase (I) and quadrature (Q) components in the transmitted wave signal, permitted measurements of the time-variation in the plasma line density and the first direct comparison in the near-field plasma density to fluctuations in overall discharge current.

II. Background Theory and Analysis

For collisionless plasmas, the path-integrated electron density can be determined from the phase shift experienced by a microwave beam transmitted through the plasma, when referenced to the phase of the same source in the absence of the plasma. The phase difference between these two signals $\Delta\phi$, resulting from the real component of the complex refractive index of the plasma, is related to the path-averaged electron density by [6]:

$$\bar{n}_e = \frac{4\pi m_e \varepsilon_o c^2}{e^2 \lambda_o \ell} \Delta\phi \quad (1)$$

Here m_e is the electron mass, e is the electron charge, c is the speed of light, λ_o is the free space microwave wavelength, ε_o is the free-space permittivity and ℓ is the path-length traversed by the microwave through the plasma. In writing Eq. 1, we assume that the magnetization of the electrons is negligible in their response to the microwave field, i.e., that the microwave frequency is much greater than the electron cyclotron frequency (which, at the exit of a Hall thruster, ranges from $10^8 - 10^9$ s⁻¹). Although a measurement of this sort is averaged along the path of microwave propagation through the plasma, co-axial Hall thrusters are reasonably axisymmetric, with annular discharge channels, so that radial variations in the plasma density can be reconstructed from a series of measurements made along paths passing through various chords of the plume. This reconstruction is facilitated by standard inverse transform methods (e.g., Abel transformations) or numerical “onion peel” techniques such as those commonly used in optical absorption spectroscopy for characterizing symmetric emission sources. In a ground test facility, the Hall thruster can be translated in the axial and radial dimensions, allowing the microwave beam to pass through many sections of the plasma column.

A schematic (block) diagram of the phase-bridge interferometer configuration used in this study is shown in Fig. 1(a). This configuration is similar to that used recently by Kawahata et al., to characterize the plasma density distribution in a Large Helical Device [7]. In the experimental arrangement employed here, the output from a 90 GHz fixed frequency Gunn diode with integral oscillator (Millitech model GDM-10-0017IR) having a 50 mW maximum output power is split into two arms of equal strength through the use of a high directional coupler (Millitech model CSS-10-R090BZ). One arm leads to two variable phase shifters (Millitech models VPS-10-R000N) providing a combined 360° phase shift, and level set attenuator (Millitech model LSA-10-R000N). The phase shifters and attenuator serve as a means of calibrating the interferometer prior to pumping down the vacuum chamber and igniting the plasma discharge. The beam is launched into the plasma through a standard pyramidal gain horn (Millitech Model SGH-10-RP000) and custom designed matched Teflon lens (50 cm focal length) with an estimated beam waist of 7 mm (diameter), characterized by introducing an attenuating target at the beam focus during the beam alignment process. The beam is collected with a second matched lens/horn combination. Both the return arm from the collection horn, and the second arm originating at the diode, are split further into two equal sources with two more highly directional couplers (Millitech model CSS-10-R090BO). The two pairs of source (incident) and return arms are combined in two independently balanced and biased mixers (Millitech model MXB-10-RR0WX). The mixers serve as wave multipliers with low-pass filters, having a DC-510 MHz IF frequency response. All components of the microwave circuit are coupled through the use of sections of non-standard length WR-10 waveguides. Figure 1(b) provides a more detailed illustration of the experiment, and depicts the positioning of both horns and lenses relative to the Hall discharge.

For an incident wave $S_i(t) = A_1 \cos(\omega t)$ and transmitted wave $S_r(t) = A_2 \cos(\omega t + \Delta\phi)$, the mixer output gives a DC signal proportional to the phase shift $\Delta\phi$ (so-called *In-phase* component, or *I*-signal) introduced by the plasma:

$$I = \frac{A_1 A_2}{2} \cos \Delta\phi \quad (2)$$

The source from one arm is passed through a 90° phase shifter. For the branch that includes the 90° phase shifter (the so-called *Quadrature* component), the mixer signal is:

$$Q = \frac{A_1 A_2}{2} \cos\left(\frac{\pi}{2} - \Delta\phi\right) = \frac{A_1 A_2}{2} \sin(\Delta\phi) \quad (3)$$

The ratio of the two signals generated in the balanced mixers, $R = I/Q = \tan(\Delta\phi)$. For small phase shifts, where $\tan(\Delta\phi) \approx \Delta\phi$, this ratio is ideally equal to the phase shift, since the signal amplitudes cancel. In principle, fluctuations in the output of any single mixer signal are proportional to the fluctuations in the plasma density. The ratio of the mixer outputs therefore directly corresponds to fluctuations in the plasma density.

In practice, the combined branches that give rise to the I and Q signals have unequal intrinsic losses (for example, due to differing waveguide properties and lengths, amongst others). Furthermore, the two mixers themselves may have a different sensitivity to signals at their inputs (α_I , α_Q) and an intrinsic DC offset (I_o , Q_o). As a result, the mixer signals can be represented as:

$$I = I_o + \alpha_I \frac{A_1 A_2}{2} \cos \Delta\phi \quad (3a)$$

$$Q = Q_o + \alpha_Q \frac{A_1 A_2}{2} \sin \Delta\phi \quad (3b)$$

The signals I and Q trace an ellipse in Cartesian space (Smith circles), the center of which is located at position (I_o , Q_o), as illustrated in Fig. 2. In general, a non-zero reference (no plasma) phase shift ϕ_o can arise due to intrinsic phase shifts between the two paths. In Fig. 2, the calibration (Smith) circle is shown for successive 5-degree settings in the variable phase shifter. In this figure, the calibration circle has not been re-scaled for this intrinsic phase shift and DC-offsets. It is noteworthy that the plot is not circular,

indicative of the difference in the sensitivity of the two mixers. Figure 3 provides a series of Smith circles obtained while varying the attenuators by 5 dB intervals. In this figure, the calibration circles have been re-scaled for DC offsets and intrinsic phase shift (to the 0 dB circle). Note that although an attenuation of much less than 1 dB is expected for the collisionless plume of this discharge, these calibration circles indicate that the variable attenuator does introduce an added phase shift which would have to be corrected for when probing collisional plasmas. All results presented here use zero-attenuation calibration circles for data reduction – i.e., we assume that the plasma plume in the near-field is collisionless.

It is noteworthy that with the entire interferometer located within the vacuum chamber, the intrinsic heat dissipation from the powered mixers and diodes (as well as some heat loading from the plume/thruster), introduces noticeable (but abrupt) drifts in the phase, and offsets in the mixers. These drifts precluded the measurements of plasma line-density to no better than a factor of about two. Higher accuracy and reproducibility will require active cooling of the components while operating in vacuum - changes which we are currently implementing [8]. Modifications are also planned for in-situ calibration of the interferometer in vacuum. In this paper, calibrations are carried out prior to the sealing and evacuation of the chamber.

Because of these possible drifts in the zero-phase reference, our analysis could not rely on the identification of the precise location of the I and Q signals on the ex-situ calibrated Smith circles. Instead, an alternate approach to data reduction is taken. The analysis of the data for the results presented here is relatively straightforward, and relies on identifying (experimentally), a zero-phase shift reference point by recording mixer signals (I_{op} , Q_{op}) with the microwave beam passing through regions of the plume where there is little/no plasma. For the small phase shifts anticipated when passing through the near-field plume ($< 5^\circ$), the arc swept along the Smith circle from this zero-phase shift condition, $S = [(I-I_{op})^2 + (Q-Q_{op})^2]^{1/2} = M \Delta\phi$. Here, M is the modulus in the mixer signal at zero-phase, corrected for the DC offset: $M = ((I_{op}-I_o)^2+(Q_{op}-Q_o)^2)^{1/2}$. The phase shift (and hence plasma density from Eq. 1) is determined then, from:

$$\Delta\phi = \frac{S}{M} = \frac{\left([I - I_{op}]^2 + [Q - Q_{op}]^2\right)^{1/2}}{\left([I_{op} - I_o]^2 + [Q_{op} - Q_o]^2\right)^{1/2}} \quad (4)$$

A representative scan of the $I-I_{op}$, and $Q-Q_{op}$ signals obtained as the thruster is traversed across the microwave beam at an axial position of $z = 95$ mm ($z = 0$ mm is the location of the exit plane) is shown in Fig. 4. The resulting lateral variation in signal S is shown in Fig. 5. An estimate of the modulus, M , for the mixer signal at zero phase in the absence of the plasma, obtained from a calibration circle carried out prior to the measurements, is $M \approx 60$ mV. The measurement of S along with M is used to determine the phase shift, which would have a lateral distribution similar in shape to the signal depicted in Fig. 5.

III. Experiment

The measurements were carried out at the Air Force Research Laboratory (Edwards Air Force Base, CA) Hall thruster test facility (Chamber Six). A three-dimensional illustration of the interferometer assembly as constructed on a rigid-frame structure and installed into the vacuum chamber is shown in Fig. 6.

The Hall discharge plasma thruster studied here (BHT-200) is a commercial plasma thruster developed by Busek Co. (Natick, MA). The nominal discharge power is approximately 200W. The thruster is a typical co-axial design (see Fig. 1b)), with a boron nitride annular channel and an inner and outer wall diameter of 14 mm and 31 mm respectively (8 mm channel width). The central pole piece (also covered with a conical boron nitride cap) extended approximately 7 mm beyond the exit plane of the channel. The magnetic field is mostly radial in direction near the channel exit, generated by the inner and outer magnetic pole pieces, and falls off rapidly with axial position downstream of the exit plane. The channel exit served as the origin position marker for the axial (z) position referred to in the measurements. The cathode (which also operates on xenon flow) was located approximately 20 mm downstream of the central pole piece. Further details of the design of this plasma accelerator can be found in Ref. 5.

The vacuum chamber in which the plasma thruster is operated in is 1.8 m in diameter and 3 m long with a measured pumping speed of approximately 32,000 l/s on xenon, provided by four single-stage

cryogenic panels and one 50 cm diameter two-stage cryogenic pump. The thruster was operated at nominal conditions of 0.8 A of discharge current, 250V discharge voltage (controlled mode), an anode mass flow rate of 8.5 sccm, and a cathode mass flow rate of 1 sccm.

IV. Results

Measurements were made at nominal discharge operating conditions while translating the Hall thruster through a range of axial (z) and lateral positions so that the focused microwave beam passes across a chord of the plume, in a plane normal to the z -direction. Mixer signals were recorded digitally, and the signal modulus S and reference modulus M were then used to determine the phase shift and plasma line-density, $\bar{n}_e \ell$. The variation in this line-density with lateral position is shown in Figure 7. If we were to use the typical width of the distribution shown as a path length (~ 50 mm), then the average plasma density across this 50 mm path length is about $2 \times 10^{17} \text{ m}^{-3}$, consistent with what is expected in the very near field (within one engine diameter) of this Hall thruster, and (to within an order of magnitude) with the probe measurements of Beale, et al [9].

The lateral profiles in Fig. 7 hint to the possible presence of a dip in the plasma density along the axis. Measurements were also taken at a fixed lateral position corresponding to chords passing through the axis of the thruster and varying axial positions. The variation in the plasma line-density with axial position is shown in Fig. 8. During the first 50 mm, the line density is seen to fall exponentially with axial position from the exit plane of the thruster, leveling off between 50 and 60 mm, clearly suggesting the presence of a feature at this location. We have found that in the very near field (e.g., < 10 mm), interferences with the microwave beam are introduced, perhaps by the placement of the cathode, or by the protruding central nose cone. It is noteworthy that at larger axial positions, there is an apparent asymmetry, which we attribute to the cathode jet. Also, axial positions closer than 10 mm from the exit plane introduce further complications in the interpretation of the data, as the beam waist becomes comparable to the channel

width of the thruster. No attempt has been made here to deconvolve the beam waist from the lateral data. Therefore, the features shown in the lateral and axial profiles are expected to be sharper than indicated.

Figure 9 is an Abel inversion of the data, with interpolation applied to provide a smooth color mapping for visualization of the plasma density field. The inversion is carried out on the lateral half of the data opposite the side of the cathode placement (negative lateral positions in Fig. 7, bottom map in Fig. 9) and on the side of cathode placement (positive lateral positions in Fig. 7, top map in Fig. 9). The Abel inverted images are superimposed onto a photograph of emission from the thruster, which is also shown above and below the images respectively, for comparison. The inverted data reveals the presence of a plasma torus very near the exit plane of size comparable to the discharge channel. This is expected, as the plasma will be most dense where it exits from the annular channel. However, the inverted image also reveals a more complex ion flow field further downstream, with a very low density region near the beam convergence, followed by region of concentrated plasma near the axis, some 50-55 mm downstream of the discharge exit. It is noteworthy that this near-field structure is not revealed in the triple-probe measurements of the same discharge, in Ref. 9.

This interferometer also provides a non-intrusive means of characterizing temporal fluctuations in the plasma density. For small phase shifts, the output from a single mixer will have a temporal component that is proportional to the fluctuations in the plasma line-density. In the vicinity of the exit plane, large-scale fluctuations are attributed to the so-called “breathing” mode of Hall discharges [10], which arises as a result of the competition between rapid depletion of mass within the channel due to ion acceleration, and the replenishing of xenon through anode injection. This large scale fluctuation is usually identified through analysis of the temporal fluctuation in the discharge current. However, such a “global” parameter may not necessarily reflect the behavior of the discharge at a particular position, such as the exit plane or near-field of the thruster.

Figure 10 below compares the Fourier spectrum of the discharge current fluctuations to the fluctuation in plasma density seen along a central chord at an axial position of $z = 10$ mm from the exit

plane. Apparent in both traces is the relatively strong principal oscillation at about 17 kHz, along with four harmonics. There is a remarkable similarity between the two traces depicted in the figure, which implies that the low-frequency large scale oscillations in the plume plasma density (near-field) is indeed representative of the breathing mode that is ubiquitous in the low frequency oscillations in discharge current.

The microwave diagnostic permits the non-intrusive recording of high frequency ($\gg 100$ kHz) disturbances in the near field of the thruster, which, prior to this, have been characterized nearly exclusively by intrusive probes. The only drawback associated with the application of microwave interferometry to study these fluctuations is that it is a line-of-sight diagnostic, and will resolve only those disturbances that are of relatively large scale – possibly azimuthal waves limited to wavelengths larger than a few centimeters. A study of these high frequency oscillations will be reported in a future paper.

V. Summary

The structure of the near-field plasma in the plume of a commercial 200W Hall thruster is elucidated through spatially-resolved measurements of electron density using millimeter wave interferometry. The 90 GHz beam is focused down to a waist of approximately 7 mm, and over a 50 mm plasma path length, easily measurable 3° phase shifts are recorded. The system is of a phase-bridge design, utilizing two signal arms split from a fixed frequency source (one passing through the plasma) that recombine at two balanced mixers. A path-integrated electron density is obtained by comparing the two signals from the mixers. Abel inversion is used to convert the path-integrated density to radial variations across the discharge exit. The plasma density near the exit plane is found to be $\sim 4 \times 10^{17} \text{m}^{-3}$, consistent with that measured at the exit plane of other Hall discharges [3], and in the shape of a torus, resembling the annular discharge channel. The plasma torus appears to converge revealing the persistence of a low density jet along the discharge axis (characteristic of the bright conical emission seen in emission). An additional rise in density follows some 50 mm downstream of the exit plane, on axis – structure or behavior not captured in recent probe studies [9]. This interferometer is shown to be suitable for measuring time-

dependent plasma density fluctuations offering unprecedented information about plasma fluctuations in the near exit region, and the opportunity to study turbulence-enhanced electron transport in regions where the plasma is presumably collisionless and free of interactions with the channel wall.

Acknowledgements

This research was supported by the Air Force Research Laboratory and the Air Force Office of Scientific Research. Partial support for M.C. was provided through a Summer Fellowship from the National Academy of Science. Support for N.G. was provided through a post-doctoral fellowship from the European Space Agency. The authors would like to acknowledge Mr. Wes Hermann, who was instrumental in the assembly of the initial instrument, Mike Kodiak, who carried out calibrations and assisted in the first application of the interferometer at AFRL, and T. Cote, at Millitech, who offered many suggestions in the early phases of the development of the interferometer.

References

1. W.A. Hargus, Jr., and M.A. Cappelli, "Laser-induced fluorescence measurements of velocity within a Hall discharge," *App. Phys. B: Lasers and Optics*, **72**, 961, 2002.
2. A.M. Bishaev and V. Kim, "Local plasma properties in a Hall current accelerator with an extended acceleration zone," *Sov. Phys. Tech. Phys.* **23**, 1055, 1978.
3. N.B. Meezan and M.A. Cappelli, "Anomalous electron mobility in a coaxial Hall discharge," *Phys. Rev. E* **63**, 026410-1, 2001.
4. B. E. Gilchrist, S. G. Ohler, and A. D. Gallimore, "Flexible microwave system to measure the electron number density and quantify the communications impact of electric thruster plasma plumes," *Rev. Sci. Instrum.* **68**, 1189, 1997.
5. W.A. Hargus, Jr. and G. Reed, "The Air Force clustered Hall thruster program," AIAA-2002-3678, 38th Joint Propulsion Conference, July 7-10, Indianapolis, IN, 2002.
6. M. Mitchner and C.H. Kruger, Jr., in *Partially Ionized Gases* (John Wiley and Sons, New York), 1973, p. 161.
7. K. Kawahata, K. Tanaka, T. Tokuzawa, Y. Ito, T. Akiyama, A. Sanin, S. Okajima, S. Tsuji-Iio, and L. Vyacheslavov, "Electron density profile measurements on LHD", *IEEE Trans. on Plasma Science* **32**, 519, 2004.
8. G. Reed, W. Hargus, and M. Cappelli, "Microwave interferometry (90 GHz) for Hall thruster plume density characterization," AIAA-2005-4399, 41st Joint Propulsion Conference, July 10-13, Tucson, AZ, 2005.
9. B. E. Beal, A. D. Gallimore, and W. A. Hargus Jr., "Plasma properties downstream of a low-power Hall thruster," *Phys. Plasmas* **12**, 123503, 2005.

10. E.Y. Choueiri, "Plasma oscillations in Hall thrusters, Phys. Plasmas, **8**, 2001.

Figure Captions

Figure 1. (a) Schematic diagram of the phase-bridge interferometer. 1-90 GHz Gunn Diode, 2- Splitters, 3- Balanced Mixers, 4 – Variable Attenuator, and 5 – Variable Phase Shifter. (b) Schematic illustration of the thruster and focused microwave beam. In the actual experiment, the cathode placement is out of the plane of the microwave beam.

Figure 2. (color on-line) Smith diagram of the microwave interferometer response, obtained by varying the phase setting in the phase shifters (not re-scaled for intrinsic phase shifts and offsets).

Figure 3. (color on-line) Smith diagram of the microwave interferometer response, obtained by varying the phase setting in the phase shifters and attenuation settings in the variable attenuator. (re-scaled for intrinsic phase shifts and offsets).

Figure 4. (color on-line) I and Q mixer signals obtained as thruster is traversed across microwave beam.

Figure 5. (color on-line) Signal, S corresponding to the arc swept along the Smith circle as the plume traverses the microwave beam.

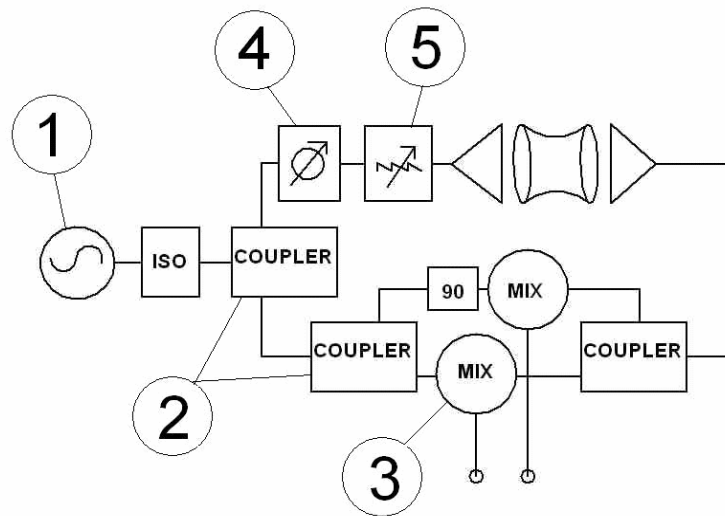
Figure 6. (color on-line) 3D depiction of the phase - bridge interferometer. 1-90 GHz Gunn Diode, 2- Splitters, 3- Balanced Mixers, 4 – Variable Attenuator, and 5 – Variable Phase Shifter.

Figure 7. (color on-line) Typical results of plasma line density versus lateral position at various axial position obtained. The exit plane is at $z = 0$ mm. Positive lateral positions correspond to the side where the cathode is located. These data have not yet been inverted.

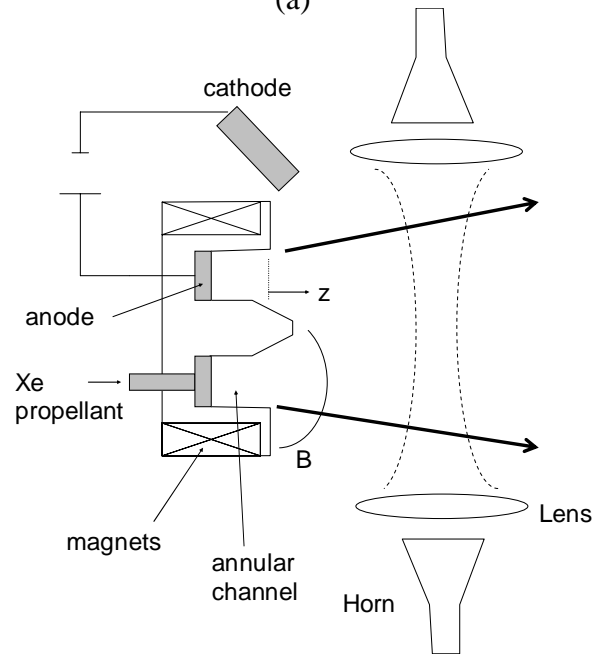
Figure 8. (color on-line) Axial variation in the plasma line density in the Hall discharge plume. The exit plane is at $z = 0$ mm.

Figure 9. (color on-line) (a) Photograph of the Hall thruster plasma. (b) Color mapping of Abel inverted data of Fig. 7 – plasma density variation with radius, superimposed onto the photograph for scale reference. The top map is the inversion of lateral data on the cathode side. The bottom map is the inversion of lateral data opposite the cathode side. The limit on the color scale is $3.5 \times 10^{17} \text{ m}^{-3}$.

Figure 10. (color on-line) Fourier decomposition of the discharge current (top) and microwave mixer signal (bottom) with the microwave beam passing through the near field ($z = 10 \text{ mm}$).



(a)



(b)

Fig. 1. Cappelli et al.

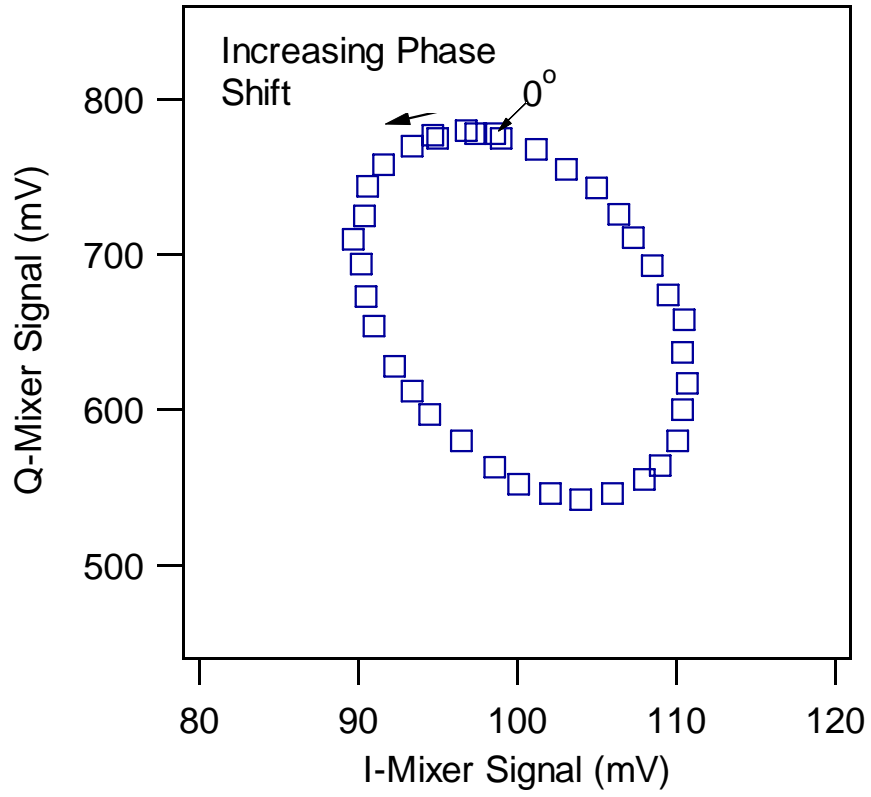


Fig. 2. Cappelli et al.

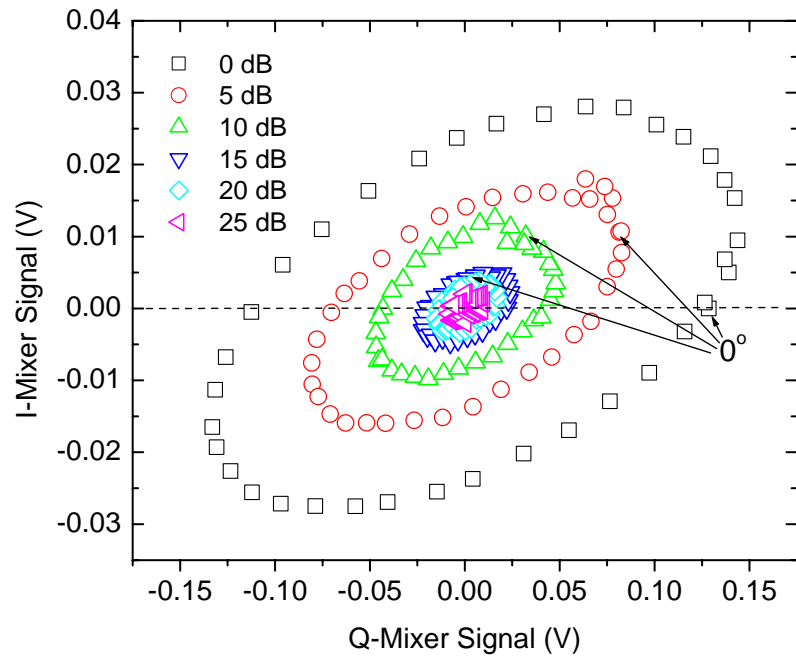


Fig. 3. Cappelli et al.

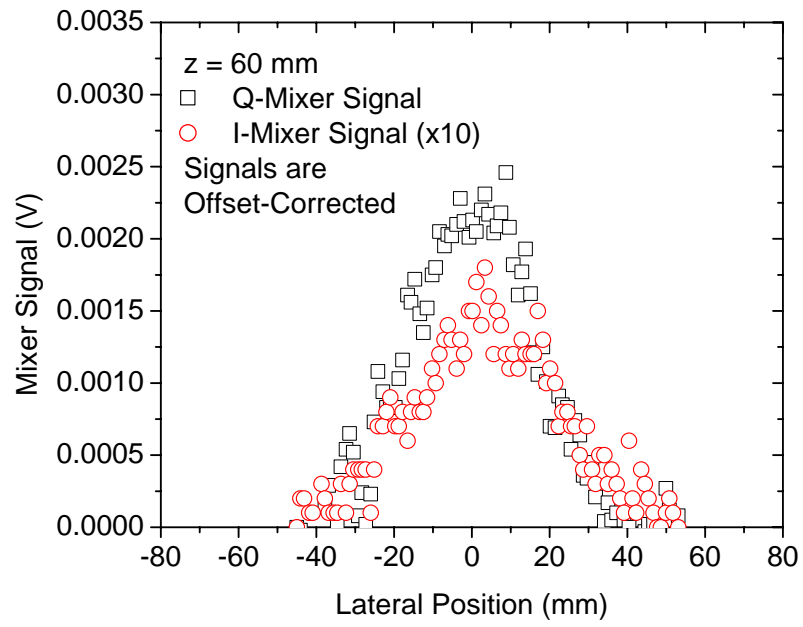


Fig. 4. Cappelli et al.

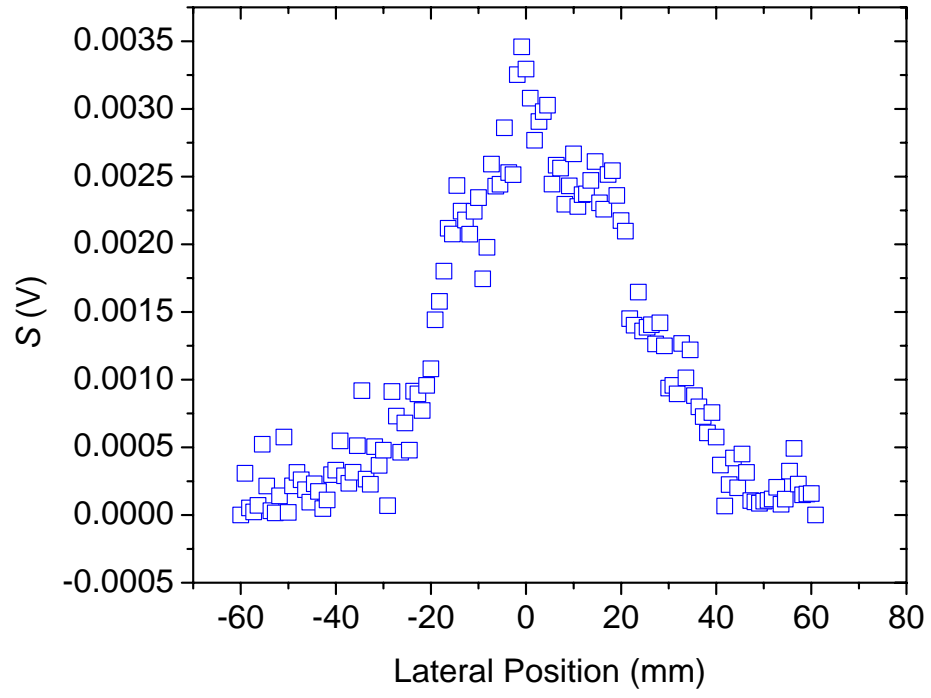


Fig. 5. Cappelli et al.

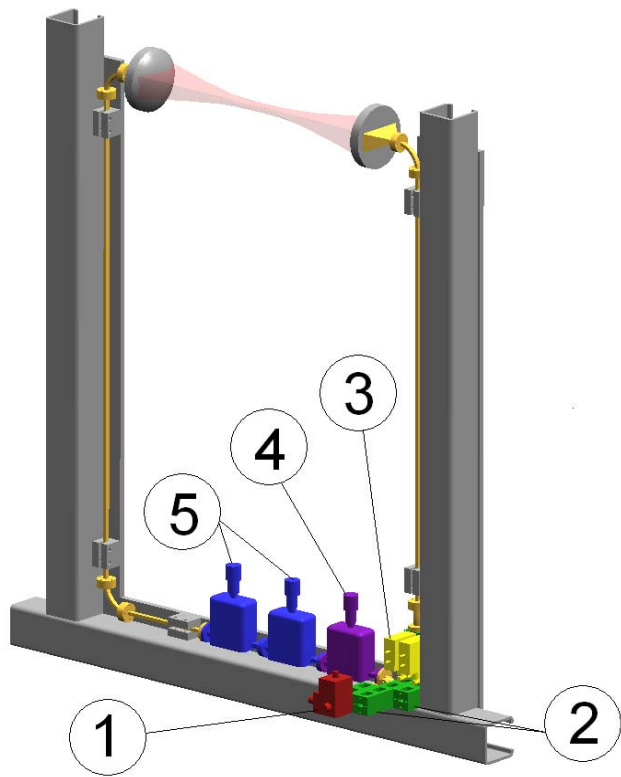


Fig. 6. Cappelli et al.

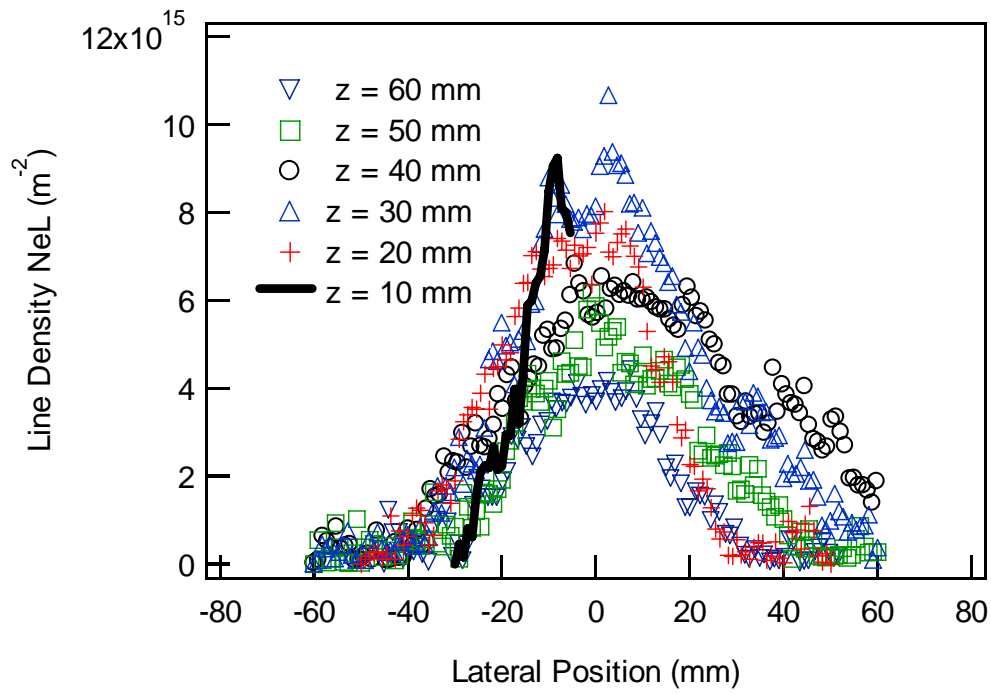


Fig. 7. Cappelli et al.

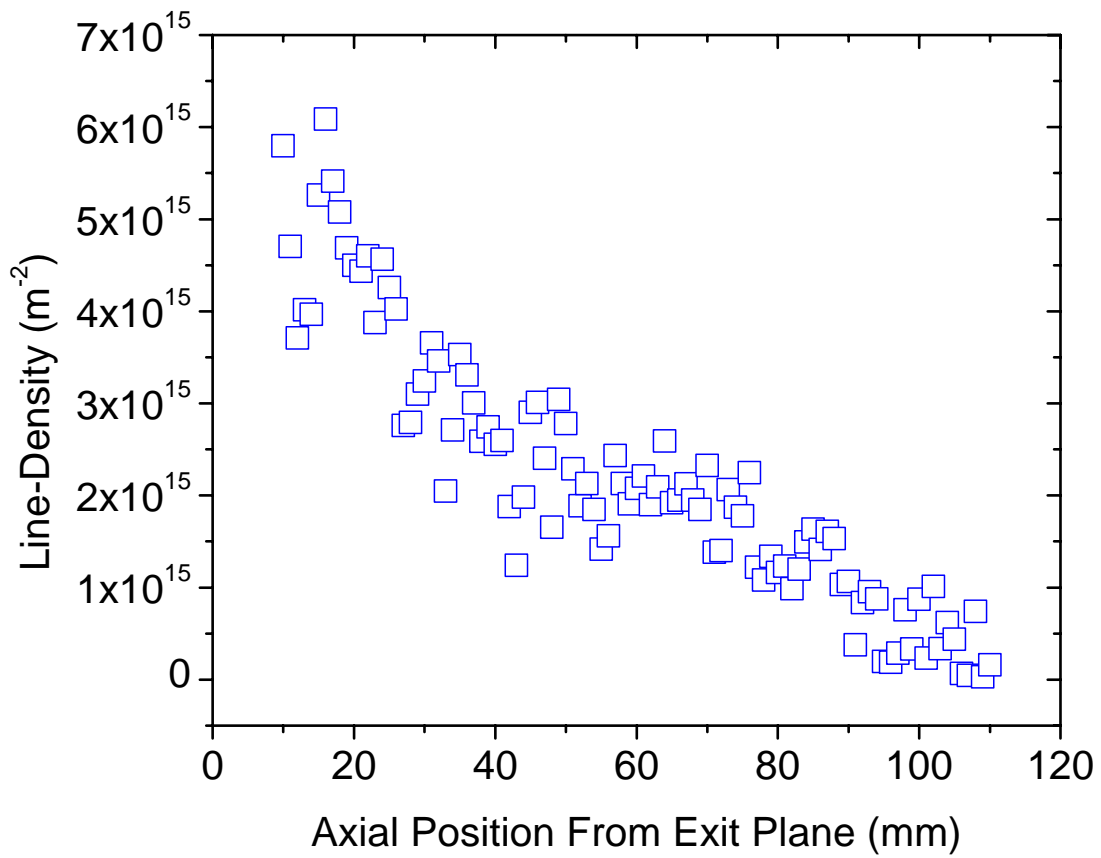
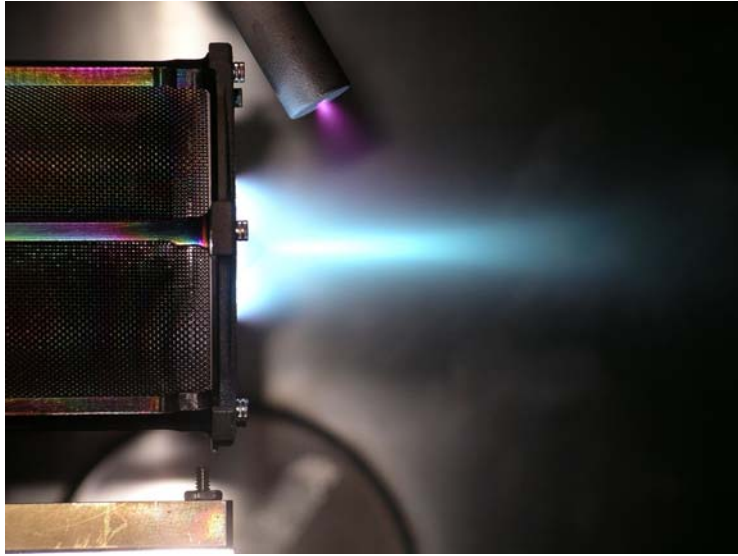
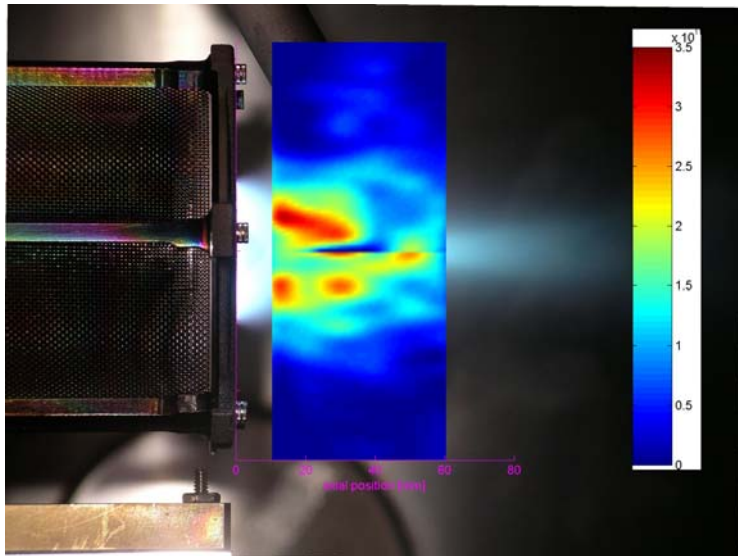


Fig.8. Cappelli et al.



(a)



(b)

Fig. 9 Cappelli et al

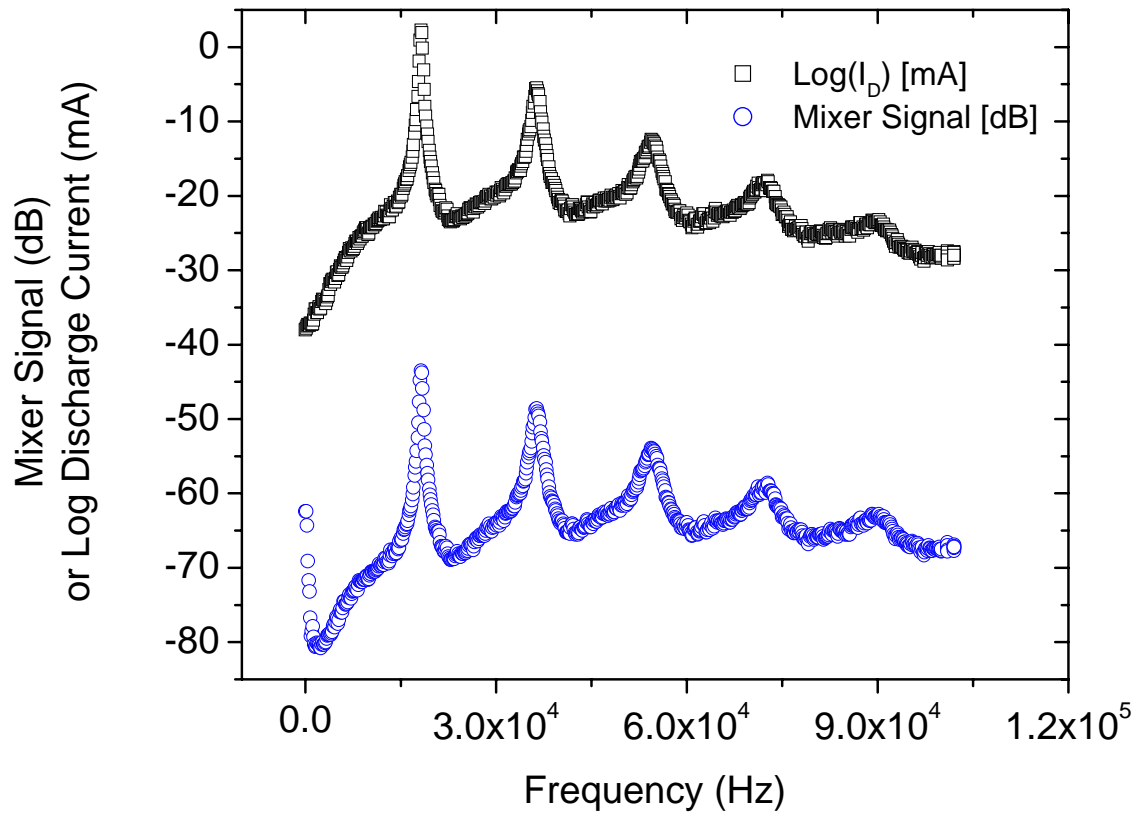


Fig.10. Cappelli et al